Effects from Metal Ion in Tumor Endothelial Marker 8 and Anthrax Protective Antigen: BioLayer Interferometry Experiment and Molecular Dynamics Simulation Study

Zhe Jia,[a] Christine Ackroyd,[b] Tingting Han,[a] Vibhor Agrawal,[a] Yinling Liu,[a] Kenneth Christensen,*[b] and Brian Dominy *[a]

One of the anthrax receptors, tumor endothelial marker 8 (TEM8), is reported to be a potential anticancer target due to its over-expression during tumor angiogenesis. To extend our BioLayer Interferometry study in PA-TEM8 binding, we present a computational approach to reveal the role of an integral metal ion on receptor structure and binding thermodynamics. We estimated the interaction energy between PA and TEM8 using computer simulation. Consistent with experimental study, computational results indicate the metal ion in TEM8 contributes significantly to the binding affinity, and PA-TEM8 binding is more favorable in the presence of Mg^{2+} than Ca^{2+}. Further, computational analysis suggests that the differences in PA-TEM8 binding affinity are comparable to the closely related integrin proteins. The conformation change, which linked to changes in activity of integrins, was not found in TEM8. In the present of Mg^{2+}, TEM8 remains in a conformation analogous to an integrin open (high-affinity) conformation. © 2017 Wiley Periodicals, Inc.

DOI: 10.1002/jcc.24768

Introduction

Since the bioterrorism attack in 2001, the need to understand and develop countermeasures for anthrax virulence has drew significant attention.[1] The infectious agent is typically transmitted through ingestion, inhalation, or cutaneous, followed by infection at the site of contact, causing distinct clinical symptoms.[2] Amongst the virulence mechanisms utilized by *Bacillius anthracis*, production of the binary toxin proteins occurs throughout the vegetative life stage of the pathogen. The mechanism of anthrax intoxication begins when anthrax protective antigen (PA), a component of anthrax toxin, binds to anthrax toxin receptors on the cell surface.[3]

Tumor endothelial marker 8 (TEM8) is one of the anthrax cell surface receptors in humans.[3] PA binds to TEM8 and interacts with the other toxin proteins, lethal factor, and edema factor, to facilitate internalization and delivery of the lethal and edema factors via endocytosis and pore formation.[4] TEM8 is also known to be over-expressed in tumor cells,[3] and is originally identified as the product of gene upregulation in tumor endothelium.[5] Since TEM8 functions in angiogenic processes that can enhance tumor growth,[6,7] the receptor has generated much interest as either a cancer marker[8,9] or a target for tumor-specific therapies.[9]

X-ray crystallographic studies[4] demonstrates that TEM8 is a von Willebrand factor type A protein that contains a divalent cation in a metal ion dependent adhesion site (i.e., the MIDAS domain). Most other von Willebrand factor A proteins, including integrins, bind their relevant physiological ligand(s) via the metal cation. TEM8 mutants that disrupt metal binding, or wild-type TEM8 that lacks the divalent metal, yield a significant decrease in PA-TEM8 binding affinity.[10] Biological experiments show that a mutated version of PA inhibits angiogenesis *in vivo*. Thus, PA is believed to occupy the same binding site as physiological extracellular membrane ligand(s).[11] Consequently, PA-TEM8 interactions may be reasonably used as a model for studying TEM8 binding behavior both to its physiological ligand and anthrax protective antigen, to modulate the angiogenic effect(s) of TEM8 and the anthrax infection pathway. However, the exact structure of PA-TEM8 complex and the molecular mechanism by which TEM8 exerts its angiogenic effect remain unclear.

Another anthrax receptor, capillary morphogenesis gene 2 (CMG2), shares 40% amino acid identity with TEM8, with close to 60% identity in the PA binding domain. Further, the affinity between the anthrax receptor CMG2 and PA is significantly affected by the identity of the bound metal cation.[12] Three possible metal ions facilitate the binding by coordinating to the MIDAS domain in CMG2: Mg^{2+} has the strongest binding affinity, followed by Zn^{2+}, and then Ca^{2+}.[12,13] Similar results are found for TEM8.[14] However, a systematic examination of the role of the divalent cation on the PA-TEM8 interaction has not been carried out.

In addition, several groups have also recognized the structural similarity between integrin α I domain and TEM8 extracellular domain. They speculate that the binding of TEM8

[a] *Z. Jia, T. Han, V. Agrawal, Y. Liu, B. Dominy*
Clemson University Department of Chemistry, 309 Hunter Lab Clemson University, Clemson, South Carolina 29634
[b] *C. Ackroyd, K. Christensen*
Department of Chemistry and Biochemistry, C205 BNSN, Brigham Young University, Provo, Utah 84602
E-mail: kenc@chem.byu.edu; dominy@clemson.edu
Contract grant sponsor: National Science Foundation Career Award (to B. N. D.); Contract grant number: MCB-0953783
© 2017 Wiley Periodicals, Inc.

cytosolic domains to actin can result in conformational changes that switch the TEM8 MIDAS domain from high to low affinity states, and that these two conformational states could resemble the "open" and "closed" conformations of integrin MIDAS domains, respectively.[15,16] Presumably, such conformational changes could be responsible for TEM8 signaling. TEM8 X-ray structures show more similarity to the integrin α I domain "open" conformation than to the "closed" conformation. Many integrin α I domain crystal structures are always bound to a ligand in "open" conformation, and not bound to a ligand in "closed" conformation. Although the TEM8 crystal structure does not contain a ligand, the published structure is believed to be an "open" conformation.

The integrin α conformation change is believed to be strongly coupled to the conformation of a phenylalanine on the C-terminal and a tyrosine near the MIDAS domain.[17] F205 and T118 are the corresponding residues conserved in TEM8, versus the phenylalanine and tyrosine in integrin α. Mutation of the TEM8 phenylalanine 205, highly conserved among related integrins, to tryptophan (F205W) has been speculated to lock TEM8 into a high affinity state. Conversely, the T118A mutation lowers the binding affinity to PA by ~103 fold.[18]. However, no structural data directly supporting different conformational states has been generated for TEM8, and only small differences in TEM8 affinity for PA have been observed for the F205W mutation.[18]

To investigate the role of the metal ion in the TEM8 and PA interaction, we generated a PA-TEM8 complex structure model based on the highly homologous PA-CMG2 crystal structure and evaluated the molecular model in the presence of different divalent cations. We also used our model to examine the possibility of "open" to "closed" conformational change previously suggested for TEM8.[15,18] To validate the computational model, we measured binding affinity through BioLayer Interferometry (BLI) experiments that focused on the PA-TEM8 interaction in the presence of Mg^{2+} and Ca^{2+}. We found the molecular reason for the difference in binding affinity between PA and TEM8, the "hot-spot" residues that contribute most to PA-TEM8 affinity, and examined the possibility of a TEM8 "open" to "closed" conformation change.

Methods

Preparation of complex

To model PA-TEM8 complex, we used a rigid body structural alignment TOPMATCH[19] to replace the CMG2 in the crystal structure of PA-CMG2 complex (1T6B[20]) with TEM8 (3N2N[10] chain A) at RMSD = 0.66 Å. Missing loops in PA were patched using the optimized conformation generated by Modeller9.11.[21] To reduce the computation cost, PA domain I and III were truncated in the simulation. The effect of the truncation is evaluated in Supporting Information Figure S1. Mg^{2+} ion was found in the original crystal structure of TEM8.[10] To study the effects of different metal ions, we replaced the Mg^{2+} with Ca^{2+}, and set their initial coordinates as the same as Mg^{2+}.

To model free TEM8, the crystal structure of the TEM8 monomer chain "A" was used. Ion replacement, energy minimization and molecular dynamics were done in the same way as PA-TEM8 complex, but without restraints.

Molecular dynamics simulation

The first minimization was conducted before dissolving the protein in explicit solvent to remove energy clashes. The initial atomic coordinates of PA-TEM8 complexes were dissolved in a generalized Born implicit solvent with 0.15 mol·L^{-1} salt concentration using the CHARMM 35b6 software package[22] and charmm27 force field parameters.[23] The energy minimization has 10 cycles of 1000 steps, reducing the harmonic restraint each cycle on all protein atoms from 10 kcal·mol^{-1}·Å^{-2} to 1 kcal·mol^{-1}·Å^{-2} in decrements of 1 kcal·mol^{-1}·Å^{-2} under Steepest Descent method in CHARMM.

The protein was then dissolved in a TIP3P[24] water and 0.15 mol·L^{-1} NaCl box of 126 Å × 86 Å × 86 Å at a mixed density of 0.947 g/cm^3. Extra chloride anions were used to neutralize the positive charge of the protein complex.

After the protein solvent was generated, further energy minimization and molecular dynamics simulations of protein solution were run using NAMD 2.10-GPU software package[25] with charmm27 force field parameters. Two cycles of 10,000 steps of Conjugated Gradient minimization were run in NAMD with fixed protein atoms and without any constraints, respectively. Finally, 10 repeats of 20 ns molecular dynamics using different random seeds for starting velocities[26] were produced for PA-TEM8 and PA-CMG2 complexes. Temperature was set at 300 K with a damping coefficient of 5 ps^{-1} using Langevin dynamics.[27] Pressure was set at 1 bar using a Langevin–Noose Hoover piston[28] with a damping time of 50 ps^{-1}. Particle Mesh Ewald[29] was used to calculate long-range Coulombic interactions. The time step was set at 2 fs with the use of the Rigid Bond algorithm[30] between hydrogen atoms and heavy atoms.

MM/GBSA energy calculation

In this study, the binding free energy was calculated using a widely used MM/GBSA[31–34] method. The binding interaction energies can be estimated according to the equation $\Delta G_{MM/GBSA} = \Delta E_{MM} + \Delta G_{GB} + \Delta G_{nonpolar} - T\Delta S$, where ΔE_{MM} is the difference of gas-phase interaction energy between proteins, including the Coulombic, van der Waals, bond, angle, and dihedral energies; ΔG_{GB} and $\Delta G_{nonpolar}$ are the polar and nonpolar components of the desolvation free energy, respectively; $-T\Delta S$ is the change in conformational entropy during the binding process. E_{MM} was determined by CHARMM with 999 Å cutoff distance (essentially no cutoff), and $G_{nonpolar} = \gamma A + b$[35] was estimated from the solvent accessible surface area (A in the equation) using SASA package in CHARMM,[36] and $\gamma = 0.00542$ kcal mol^{-1} Å^{-2}, $\beta = 0.92$ kcal/mol. G_{GB} was calculated with the GBSW approach[37,38] implemented in CHARMM. Dielectric constants of 4 and 80 were used for solute and solvent, respectively. CHARMM default optimized parameters for GB-calculations[39,40] were used.

Free energies were calculated from snapshots taken from MD trajectory at commonly used[31] 5 ps intervals from 20 ns MD simulation. The first 5 ns simulation was considered as pre-equilibrium stage based on the interaction between the

protein complex and water (red line in Supporting Information Fig. S1b), thus any data from the first 5 ns simulation were not used in further analysis. The single trajectory interaction energy calculation technique was used to cancel the errors resulting from internal energy, thermal noise, and potentially inadequate configuration sampling when the energies were calculated from multiple simulations.[41]

The change in configurational entropy on binding was calculated using the Quasi-Harmonic estimation. The variance in entropic contribution ($-T\Delta S$) of PA-TEM8 in the presence of different metal ion is relatively small (0.03 kcal/mol) compared to the variance in MM/GBSA energies (2.23 kcal/mol). Experimentally, the crystal structure of solo CMG2[20,42] showed less than 1.5 Å RMSD comparing to the CMG2 in PA-CMG2 crystal structural. So did PA domain II and IV.[20,43] Therefore, to save computing time, we assume that the volumes of configuration space occupied by the ligand and protein change negligibly on association, and the $-T\Delta S$ term was not included in binding free energy calculation.

For each PA-TEM8 complex, the binding free energy of MM/GBSA was estimated as follows: $\Delta G_{bind} = G_{complex} - G_{PA} - G_{TEM8}$, where ΔG_{bind} is the binding free energy and $G_{complex}$, G_{PA}, and G_{TEM8} are the free energies of complex, PA, and TEM8, respectively. Binding free energies resulting from non-bond interactions were decomposed at the atomic level to evaluate the contribution of individual residues to the binding free energy using the method described by Zeote, Meuwly, and Karplus.[44]

Protein production

PA was produced as mutant PA^{SSSR}[45] according to previously described methods.[46] TEM8-GST was expressed in *E. coli* (T7 Express; New England Biolabs). A 50 mL overnight culture was grown in ECPM1 and was used to inoculate 5 L of ECMP1 in a 5 L bioreactor at 37°C. The culture was grown at 37°C to a density of 5 OD_{600} and then induced with IPTG at a final concentration of 0.7 mM for 3 h at 37°C. Resulting cells were harvested via centrifugation for 20 min at 5000 × *g*. The pellet was resuspended in Tris buffer (125 mM Tris pH 8, 150 mM NaCl, 0.02% Tween 20) and lysed via two passes through a Cell Disruptor (Constant Systems). Lysate was cleared by centrifugation at 3300 × *g* for 60 min. Cleared lysate was loaded onto agarose-glutathione beads (Pierce) and purified according to manufacturer instructions; beads were washed with Tris buffer and eluted with the same buffer containing an additional 10 mM glutathione and 0.2% sodium azide. Pooled fractions were concentrated via Amicon Ultra-4 centrifugation (Millipore; 10 MW cut-off) and exchanged into HEPES storage buffer (20 mM HEPES, 150 mM NaCl, pH7, 0.02% tween, 0.05% sodium azide, diluted with 20% glycerol) using a PD-10 desalting column (GE Healthcare).

BLI measurements of TEM8-GST•PA affinity

TEM8-GST affinity for PA was measured using a OCTET Red Biolayer Interferometer (Forte-Bio; Pall Life Sciences). BLI measurements were carried out according to manufacturer instructions. TEM8-GST and PA were diluted into phosphate buffer (50 mM sodium phosphate, 150 mM NaCl, 10 mg/mL BSA) with the addition of the relevant divalent cation (1 mM $MgCl_2$, 2 mM $CaCl_2$, or both; relevant concentrations were chosen as an approximation of those likely to be found *in vivo*). TEM8-GST was loaded onto a series of anti-GST sensors using 5 μg/mL TEM solutions; loaded tips were exposed to a range of PA concentrations to observe association (typically 25 to 1000 nM, with a minimum of four different concentrations), followed by observation of complex dissociation with tips in buffer. The length of association and dissociation steps varied with the identity of the divalent cation, as outlined in Table 2. Global fit to the data for all PA concentrations were used to obtain k_{on}, k_{diss}, and K_d data, using manufacturer curve fitting protocols. R^2 for all curve fits were above 0.987.

Results and Discussion

Our simulation results show that TEM8 yields a higher binding affinity to PA in the presence of Mg^{2+} than Ca^{2+}. This result is consistent with our experimental data. The metal ion in the MIDAS domain of TEM8 contributes a large part (26% to 28%) of the binding affinity. The size of the metal ion is the major factor affecting the binding affinity. Smaller metal ions interact more strongly with both protein molecules in the complex, and result in higher binding affinity.

In calculations, the change in MM/GBSA interaction energy between metal ion and PA is larger than the change in total binding free energy. Residues around the metal ion compensate part of the change in binding affinity resulted from metal ion. Four salt bridges and three hydrophobic insertions also contribute a large part of the binding affinity. The interactions are slightly different from those identified through a structural alignment study described in 2010.[10] The conformation of TEM8 is confirmed as "open," and is stabilized in "open."

In experiments, we note that PA-TEM8 affinity in the presence of either Mg^{2+} or Ca^{2+}, obtained by BLI, has been previously reported for alternate truncations of soluble TEM8.[14,18] Our K_d values agree with previous studies qualitatively, but are not identical quantitatively. For example, while our K_d in Mg (3 ± 1 nM) obtained via BLI is lower than previous SPR data obtained by Scobie et al (130 ± 46 nM)[14] and Fu et al (30 ± 9 nM).[10] Our measured K_d in Ca (570 ± 170 nM) is two-fold lower than the Scobie value (1100 ± 41 nM)). Observed differences may simply reflect different MIDAS domain truncations. However, in all cases, PA-TEM8 off-rates are slow (10^{-4}/s, as measured by Fu et al by SPR and confirmed by our own data). Previously reported SPR values result from short (3–5 min) observations of very slow complex dissociations (when reported), which could lead to inaccuracies in the resulting reported K_d values.

Mg^{2+} results in higher PA-TEM8 binding affinity than Ca^{2+}

To measure the binding interaction energy between TEM8 and PA in the presence of different metal ions, the dissociation constant was measured experimentally by BLI in the presence

Table 1. MM/GBSA interaction energy.

Energy terms (kcal/mol)[a]	Mg^{2+}[b]	Ca^{2+}[b]
ΔE_{ele}	-28.7 ± 3.8	-22.8 ± 4.1
ΔE_{vdw}	-67.8 ± 0.6	-72.6 ± 1.2
ΔG_{SA}	-13.5 ± 0.1	-13.5 ± 0.1
ΔG_{GB}	7.1 ± 3.0	7.3 ± 3.5
$\Delta E_{vdw}+\Delta G_{SA}$	-82.2 ± 0.7	-86.1 ± 1.2
$\Delta E_{ele}+\Delta G_{GB}$	-21.5 ± 0.5	-15.5 ± 0.9
ΔG_{cal}	-103.8 ± 0.9	-101.5 ± 0.9
ΔG_{exp}[c]	-12.8 ± 0.1	-10.0 ± 0.1

[a] The standard error was estimated over the mean of 10 repeats, each repeat has 3000 data points from 20 ns MD simulation. [b] Metal ion in the MIDAS of TEM8. [c] The experimental free energy is calculated from values in Table 2, including the errors.

of Mg^{2+} and Ca^{2+}. Corresponding cations were placed in MIDAS domain in simulation models. As shown in Table 1, experiments show TEM8 bound to PA in the presence of Mg^{2+} 2.8 kcal·mol^{-1} stronger than in the presence of Ca^{2+}. Simulation data shows a difference of 2.3 kcal·mol^{-1}.

Stronger electrostatic interaction ($\Delta E_{ele}+\Delta G_{GB}$) is observed in the presence of Mg^{2+} compared to Ca^{2+}. Weaker van der Waals interactions are observed in the presence of Mg^{2+}. The major difference comes from the Coulombic interaction energy; the GB energies do not show much difference. The GB energy mimics the solvation screening effect to partially cancel out about 25% of the Coulombic term. The addition of GB energy to Coulombic energy also reduces the error of electrostatic energy by more than 70%.

In BLI experiments, TEM8 shows more than 150 times higher binding affinity toward PA in 1 mmol Mg^{2+} than in 2 mmol Ca^{2+} solutions. The trend and magnitude are consistent with our theoretical results. When replacing the metal ion from Mg^{2+} to Ca^{2+}, the on rate is about fivefold lower; however, the dissociation rate becomes 100 times faster. k_{on} and k_{diss} in the Mg^{2+} and Ca^{2+} mixture are similar to the results from the Mg^{2+} solution. First, these observations indicate that TEM8 is less active toward PA when Ca^{2+} occupies the MIDAS. Second, even when TEM8 containing Ca^{2+} binds to PA, the complex is still less stable than in the presence of Mg^{2+}. Notably, while the Mg^{2+} ion stabilizes the protein complex mainly by decelerating the dissociation, it also slightly accelerates the association process.

Table 2. Experimental binding affinities between PA and TEM8.

Metal ion in PA-TEM8[a]	K_d (nM)	k_{on} (10^4/(M s))	k_{diss} (10^{-5}/s)
Mg^{2+}	3 ± 1	1.6 ± 0.1	5 ± 1
Ca^{2+}	571 ± 170	8.7 ± 1.9	500 ± 100
Mg^{2+}& Ca^{2+}	4.3 ± 0.2	1.1 ± 0.1	4.2 ± 0.3

[a] All data were obtained from a minimum of three independent BLI experiments, as described in Materials and Methods. Errors reflect standard deviations. In the presence of magnesium, data were obtained via 5-7 min association and 30–40 minute dissociation steps; in the presence of calcium alone, dramatically faster association and dissociation could be observed fully in 60 sec. Average global fit R2 for each data set was as follows: 0.997 (Magnesium data); 0.987 (Calcium data); 0.997 (data in the presence of both magnesium and calcium).

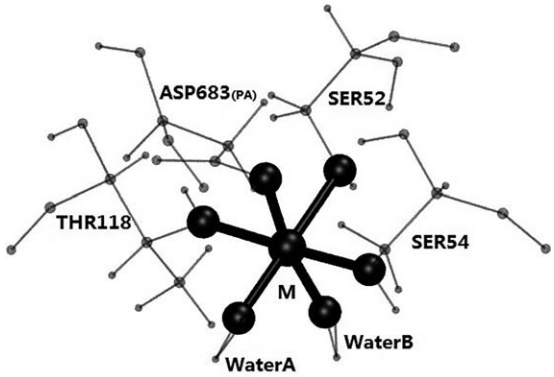

Figure 1. Diagram of MIDAS co-ordination structure in PA-TEM8 complex. M is the metal ion within MIDAS domain. THR118, SER52, and SER54 are residues on TEM8. ASP683 is a residue on PA. The metal ion and oxygen atoms involved in the coordinating have a larger size. The other atoms have a smaller size.

The calculated difference in PA-TEM8 interaction energy in the presence of Mg^{2+} and Ca^{2+} is 2.3 ± 1.3 kcal/mol, which quantitatively agrees with the experimental 2.8 ± 0.1 kcal/mol. The calculated relative interaction energy was averaged over 10 repeats of independent 20 ns simulations.

The size of metal ion matters

The distances between Mg^{2+} and all the coordinating oxygen atoms are shorter than those between Ca^{2+} and the oxygen atoms (Fig. 2). This results in Mg^{2+} interacting more strongly with the residues and water molecules around it (within 4.0 Å) than Ca^{2+} (Fig. 3). Among the three surrounding residues and the three water molecules directly bound to the metal ion in MIDAS (as shown in Fig. 1), PA-ASP683 and TEM8-SER52/54 have a larger RMSF in the presence of Ca^{2+} than Mg^{2+} (Supporting Information Table S2 and S3). The results can be interpreted as that Ca^{2+} expands the size of MIDAS domain, leading to weaker interactions with residues.

Mg^{2+} interacts more strongly with PA, TEM8, and the coordinated water molecules than Ca^{2+} in terms of both vdW and electrostatic energy (Table 3). As the distances between the metal ion and the surrounding residues increase, all interaction energies between the metal ion and PA-TEM8/Water are

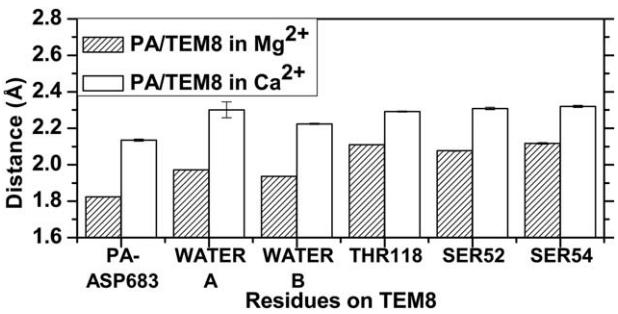

Figure 2. Distance between metal ion and the six coordinated oxygen atoms in MIDAS. The residue names are the same as shown in Figure 1. Error bars show the standard error of the means from 10 individual 20 ns MD simulations.

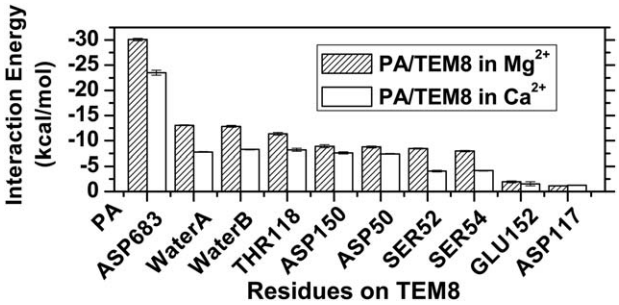

Figure 3. MM/GBSA interaction energy between metal ion and residues on PA-TEM8 complex. Residues are on TEM8 if not marked on PA. Water A and Water B are the same molecules shown in Figure 1.

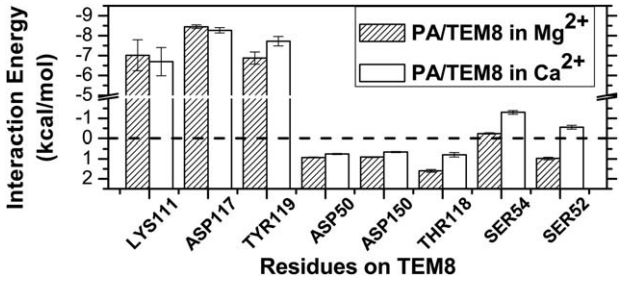

Figure 4. Largest changes in interaction energy with PA (summation of vdW, Coulombic, and Generalized Born energies) contributed by individual residues on TEM8 resulting from metal ion replacement.

weakened. This is one possible reason for the lower binding affinity in Ca^{2+} solution we observed in experiments.

The interaction energy with PA contributed by individual residues on TEM8 is also affected by the replacement of metal ion. Figure 4 shows that calculated changes on the non-MIDAS residues (LYS111, ASP117, TYR119) are smaller than the precision of the calculations, making such changes difficult to interpret. However, residues in the MIDAS domain interact more weakly with PA when Mg^{2+} is in position, compared to Ca^{2+}. This observation is opposite to the results of the interaction energy between the residues and metal ions. When Ca^{2+} is bound in the MIDAS pocket, the expanded MIDAS coordination and weakened local interaction makes the residues on TEM8 MIDAS domain interacts more strongly with PA, an effect which partly compensates for the weaker cation-TEM8 interactions.

The size of metal ion leads to the major difference in binding affinity in the presence of Mg^{2+} and Ca^{2+}. Ca^{2+} has a larger ion radius than Mg^{2+} (114 pm[47] vs. 86 pm[47]). The larger ion radius leads to a larger distance between the metal ion and the other TEM8 residues in the MIDAS domain. When the distance increased, vdW, Coulombic, and Generalized Born interaction energies became weaker, according to their definitions. Similar results were found in a quantum mechanical integrin study,[48] in which interactions between metal ions and residues within the MIDAS domain were ranked as $Mg^{2+}>Zn^{2+}>Ca^{2+}$ (the ionic radius of Zn^{2+} is between Ca^{2+} and Mg^{2+}). When expanded to PA-TEM8 complex, it follows that the smaller divalent cation interacts more strongly with both proteins in the complex, and results in higher binding affinity.

Replacing or removing metal ion possibly lead to conformation change

To further explore the reason for the different PA-TEM8 binding affinity in the presence of difference divalent cations, we simulated unbound TEM8 containing Mg^{2+}, Ca^{2+} or no metal ion in its MIDAS domain. Each simulation was 20 ns long. The crystal structure 3N2N chain A has Mg^{2+} as the MIDAS metal ion, and its MIDAS domain retained the original conformation by holding an RMSD of 0.3 Å after 20 ns (Table 4). As a substitute ion, Ca^{2+} does not fit into the MIDAS binding site as well as Mg^{2+} because of its larger ion radius; it expanded the MIDAS domain more severely than the Table 3. van der Waals, Coulombic, and generalized Born interaction energy between PA, TEM8, coordinate water and metal ions, distinction in ion size, so much so that the coordination residues cannot hold their original conformation and started to unfold. If no metal ion was present, the MIDAS domain unfolded faster than in the presence of Ca^{2+}. This agrees with the results of integrin α_L crystal structure in different metal ion conditions.[49] Unfolding was observed in all of the 10 repeats of 20 ns simulations that included either Ca^{2+} or no metal ion in the TEM8 MIDAS domain. This observation could be a result of unstable conformation(s) generated by the homology modeling method. Comparing to the structural study of integrin α_L, this result may also imply that TEM8 possesses a slightly different conformation when Ca^{2+} is present (vs. Mg^{2+}) and another obviously different conformation when there is no metal ion in the MIDAS domain.

Many integrin α I domains remain in a low affinity "closed" state in the presence of Ca^{2+}.[50] In integrin α_L, the size of the

Table 3. MM/GBSA interaction energy between metal ion and proteins.

Metal ion, Domain	$<\Delta E_{vdw}>$[a]	$<\Delta E_{elec}>$[a]	$<\Delta G_{GB}>$[a]	$<\Delta E_{elec}+\Delta G_{GB}>$[a]	$<\Delta G_{bind}>$[a]
Mg^{2+}					
PA	9.6 ± 0.1	−111.1 ± 0.3	71.7 ± 0.3	−27.1 ± 0.1	−29.8 ± 0.1
TEM8	7.2 ± 0.1	−173.4 ± 1.5	119.40 ± 1.4	−54.0 ± 0.4	−46.8 ± 0.3
Water	12.2 ± 0.1	−36.7 ± 0.1	−1.5 ± 0.1	−33.2 ± 0.1	−26.0 ± 0.1
Total	28.9 ± 0.1	−321.2 ± 0.9	189.6 ± 0.85	−114.3 ± 0.2	−102.7 ± 0.2
Ca^{2+}					
PA	9.2 ± 0.2	−106.6 ± 1.0	73.7 ± 0.97	−20.2 ± 0.1	−23.7 ± 0.8
TEM8	12.4 ± 0.3	−164.4 ± 1.4	118.4 ± 1.4	−25.8 ± 1.0	−33.6 ± 0.9
Water	11.5 ± 0.6	−26.3 ± 1.1	0.5 ± 0.2	−22.8 ± 1.2	−14.3 ± 0.7
Total	33.1 ± 0.4	−297.2 ± 1.1	192.6 ± 1.0	−68.7 ± 1.1	−71.6 ± 0.8

[a] Energies are the mean of 10 repeats ± standard error, in kcal/mol.

Table 4. RMSD of metal ions in MD simulation.

	RMSD (Å)[a]			
Metal ion in PA-TEM8	0.1 ns	0.5 ns	5 ns	20 ns
Mg^{2+}	0.3 ± 0.1	0.3 ± 0.1	0.3 ± 0.1	0.3 ± 0.1
Ca^{2+}	0.7 ± 0.2	1.1 ± 0.2	1.3 ± 0.3	1.2 ± 0.3
None	0.8 ± 0.3	1.3 ± 0.3	2.2 ± 0.2	2.7 ± 0.3

[a] All data are means of 10 repeats of 20ns simulation ± SE. RMSD are compared to the crystal structure (3N2N chain A).

metal ion was shown to affect the conformation of the MIDAS domain.[51] Although we did not observe an "open" to "closed" conformation change or location shift of F205 on TEM8 in the present of Ca^{2+}; based on the relatively lower experimental and theoretical binding affinity of TEM8 containing Ca^{2+} in MIDAS, plus the local unfolding resulting from the substitution of metal ion, we suggest that TEM8, analogous to the closely related integrin α_L, can possibly retain a low affinity conformation when Ca^{2+} is the ion in MIDAS pocket, which is slightly different from the high affinity conformation. When the metal ion is stripped out, integrin α_L suffers a moderate conformation change around the MIDAS domain, and loses most of the binding affinity toward ligand.[52] Similarly, experiments show that TEM8 loses binding affinity to PA in EDTA solution.[12] A random unfolding starting from the MIDAS domain is observed in our 20 ns free TEM8 simulation after the metal ion from MIDAS was removed (Table 4).

We suspect that TEM8 may have a different conformation in the presence of Ca^{2+} or in the absence of any metal ion in the MIDAS domain. The possible conformation change can cause larger differences in binding free energy in the presence of difference metal ions. If the protein does not unfold, results from future NMR or crystallization structural studies on TEM8 in Ca^{2+} or EDTA/EGTA can serve as powerful evidence to confirm the hypothesis.

TEM8 adopts a stabilized open conformation

A hydrophobic lock regulates the conformation change in integrin α proteins, which are 40% structurally similar to TEM8. In integrin α_M, F302 is well inserted in the hydrophobic lock when it is in the closed conformation, and it becomes exposed in open conformation (orange and cyan parts in Fig. 5A). The conversion from closed to open conformation comes with more than a 10 Å displacement on F302 in the integrin α_M.

TEM8 extracellular vWA domain (3N2N,A[10]) shows high similarity with integrin alpha I domains in open conformations. It has C_α atoms RMSD of 2.8 Å to integrin α_L (PDB ID 1MQ9[51]), 3.2 Å to integrin α_M (PDB ID 1IDO[53]), 2.71 Å to integrin α_X (PDB ID 1N3Y[54]), 2.8 Å to integrin α_1 (PDB ID 1QCY[55]), 2.8 Å to integrin α_2 (PDB ID 1DZI[56]).

The integrin I domains have two possible conformations, open and closed (Fig. 5A), representing the active and inactive states, respectively.[50] Under physiological conditions, integrins are more stable in the closed conformation than in the open conformation. The key-like residue (phenylalanine or glutamate acid, orange residue in Fig. 5A) inserts into the hydrophobic lock near C-terminal (orange cluster in Fig. 5A). In the open conformation, the key-like residue is pulled out of the hydrophobic lock, and the structure becomes less stable. The hydrophobic lock is formed by a valine (or leucine for integrin α_L) and a leucine in integrins.

In integrins, the phenylalanine (F292 in integrin α_L and F302 in integrin α_M) has a 10 times larger solvent accessible surface area in the open conformation than in the closed conformation. F292 also suffers a penalty in energy of 9–12 kcal/mol (Table 5) when integrins shift conformation from closed to open. The energy terms of TEM8 F205 are on the same magnitude as F292 and F302 in integrin α_L and α_M closed conformation.

In TEM8, F205 plays a similar role as F302 in integrin α_M and F292 in integrin α_L. In the presence of Mg^{2+} cation, the location of F205 in unbound TEM8 is more similar to the "open" conformation integrin than to the "closed" conformation (yellow residue in Fig. 5A). However, F205 in TEM8 is more buried by possessing larger solvent accessible surface area than the corresponding F302 in an integrin open conformation (Table 5), indicating that there may not be an exact TEM8 parallel of integrin "closed" or "open" conformation.

In TEM8 and CMG2, the distance between the valine and the leucine is one amino acid further (Supporting Information Table S1). As shown in the crystal structure we have for TEM8, the hydrophobic pocket is not well formed. The change in amino acid sequence around the hydrophobic pocket decreases or even reverses the energy penalty for TEM8 to stay in an "open" conformation, compared to integrins.

F205 on TEM8 interacts with the surrounding protein and solvent molecules in a manner that is more similar to "closed" conformation integrins than to the "open" conformation. Although the activity and conformation of TEM8 can be considered as "open" conformation,[10] the hydrophobic ratchet pocket controlling conformation change has 28.3 $Å^2$ solvent accessible surface area, much smaller than 161.9 $Å^2$ and 53.3 $Å^2$ for "open" conformation integrins. The hydrophobic pocket is also more stable, 9.6 kcal/mol comparing to 20.8 kcal/mol and 18.6 kcal/mol for "open" conformation integrins. Unlike

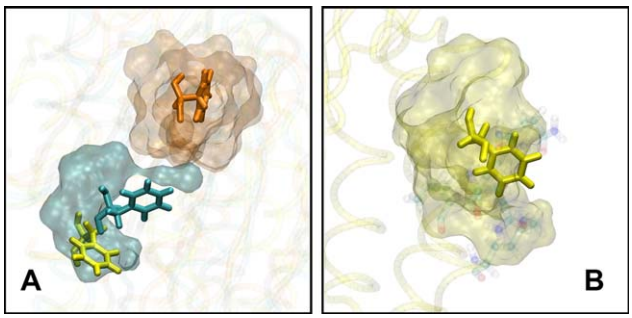

Figure 5. Comparison of the key phenylalanine on integrins and TEM8 (in Mg^{2+}) controlling conformation change. Proteins in red and cyan are integrin M in closed and open conformations, respectively. Protein in yellow is TEM8. The key phenylalanine residues (F302 on integrin M and F205 on TEM8) are highlighted. The clouds show the residues within 4.0 Å of the key phenylalanine made using 1.4 Å surface probe. (A) Comparing integrin M close and open conformation with TEM8. (B) F205 on TEM8 and the residues within 4.0 Å. [Color figure can be viewed at wileyonlinelibrary.com]

Table 5. SASA energies of hydrophobic pocket residues.

	SASA (Å^2)[a]	E_{inte}[a]
TEM8	28.3 ± 0.2	9.6 ± 0.1
α_M *open*	161.9 ± 0.3	20.8 ± 0.1
α_M *close*	13.7 ± 0.1	8.2 ± 0.1
α_L *open*	53.3 ± 0.3	18.6 ± 0.1
α_L *close*	4.0 ± 0.1	9.9 ± 0.1

[a] SASA were calculated for TEM8 F205, integrin αM F302, and integrin αL F292. Interaction energies were calculated between these residues and the rest part of the proteins. SASA and energies are the mean of 3000 frames extracted from 15 ns simulation ± SE. Energies are in kcal/mol.

the highly buried F302 and F292 in "closed" integrins or the largely exposed ones in "open" integrins, F205 in TEM8 is partially buried on the protein surface. Thus, the F205W mutation did not make a significant change in TEM8 conformation.[18] It is still possible that TEM8 has a "closed" conformation. In the presence of Mg^{2+}, however, because the TEM8 "open" conformation is more stable compared to the integrin "open" conformation, TEM8 is not likely to change to its "closed" conformation spontaneously.

Referring to the integrins, we suggest that TEM8 is in an "open" conformation, but the structural lock F205 is in a stabilized conformation closer to that of the corresponding residue in an integrin "closed" (more stable, low affinity) conformation. The TEM8 conformation can be considered as a stabilized high affinity (open) conformation.

Conclusion

Both experimental and simulation data point out that TEM8 binds to PA better in the presence of Mg^{2+} than Ca^{2+}. Because Mg^{2+} is smaller in size, it interacts with PA, TEM8, and the coordinated water molecules more strongly than Ca^{2+}, leading to higher binding affinity. Introducing Ca^{2+} to PA and TEM8 solution containing Mg^{2+} does not affect the binding affinity between PA and TEM8. This observation indicates that Mg^{2+} interacts more strongly with TEM8, in either free TEM8 or in the PA-TEM8 complex, than Ca^{2+} does. Conversely, the residues around the metal ion partially compensate the change in interaction energy by interacting more strongly to PA when Ca^{2+} is in MIDAS. The metal ion on TEM8 contributes about a quarter of the interaction energy toward PA, the rest is mostly contributed by the residues on the buried surface area.

Adding GBSA terms into traditional MM (vdw and Coulombic energies) reduces the standard deviation in interaction energy by 70%. The thermo noise mainly comes from the simulation of large contact surface area. With the help of MM/GBSA method, it is less expensive to obtain 1 kcal/mol precision for protein-protein interaction energy calculations.

We suggest the existence of a low affinity conformation of TEM8 in the presence of Ca^{2+} in MIDAS and a locally unfolded conformation in the absence of metal ion. Limited by the simulation time scale, large domain motion or conformational change is not observed in the simulation. Future structural studies are needed to provide more evidence to confirm this hypothesis.

TEM8 stays in a stabilized "open" conformation in the present of Mg^{2+}, unlike integrin α I domains, of which the "open" conformation is not as stable as their "closed" conformations. Although the overall backbone structure, binding affinity, and location of F205 all indicate TEM8 is in an "open" conformation, the SASA, and energy penalty of F205 suggest the conformation is stabilized. It is possible to experimentally obtain TEM8 in the "closed" conformation; but different from integrins, TEM8 may not change to "closed" conformation spontaneously from "open" conformation.

Keywords: TEM8 · CMG2 · biolayer interferometry · MM/GBSA · integrin

How to cite this article: Z. Jia, C. Ackroyd, T. Han, V. Agrawal, Y. Liu, K. Christensen, B. Dominy. *J. Comput. Chem.* **2017**, *38*, 1183–1190. DOI: 10.1002/jcc.24768

Additional Supporting Information may be found in the online version of this article.

[1] J. A. Young, R. Collier, *J. Annu. Rev. Biochem.* **2007**, *76*, 243.
[2] T. V. Inglesby, *JAMA* **2000**, *283*, 1963.
[3] K. A. Bradley, J. Mogridge, M. Mourez, R. J. Collier, J. A. Young, *Nature* **2001**, *414*, 225.
[4] K. A. Bradley, J. A. Young, *Biochem. Pharmacol.* **2003**, *65*, 309.
[5] B. St Croix, C. Rago, V. Velculescu, G. Traverso, K. E. Romans, E. Montgomery, A. Lal, G. J. Riggins, C. Lengauer, B. Vogelstein, K. W. Kinzler, *Science* **2000**, *289*, 1197.
[6] L. M. Cryan, M. S. Rogers, *Front. Biosci.* **2011**, *16*, 1574.
[7] A. Nanda, B. St Croix, *Curr. Opin. Oncol.* **2004**, *16*, 44.
[8] R. Raeisossadati, M. Farshchian, A. Ganji, A. Tavassoli, A. Velayati, E. Dadkhah, S. Chavoshi, M. Mehrabi Bahar, B. Memar, M. T. Rajabi Mashhadi, H. Naseh, M. M. Forghanifard, M. Moghbeli, O. Moaven, M. R. Abbaszadegan, *Int J Colorectal Dis.* **2011**, *26*, 1265.
[9] A. E. Frankel, C. Carter, S. R. Kuo, J. H. Woo, J. Mauldin, J. S. Liu, *Anticancer Agents Med. Chem.* **2011**, *11*, 983.
[10] S. Fu, X. Tong, C. Cai, Y. Zhao, Y. Wu, Y. Li, J. Xu, X. C. Zhang, L. Xu, W. Chen, Z. Rao, *PLoS One* **2010**, *5*, e11203.
[11] L. M. Cryan, K. A. Habeshian, T. P. Caldwell, M. T. Morris, P. C. Ackroyd, K. A. Christensen, M. S. Rogers, *J. Biomol. Screen.* **2013**, *18*, 714.
[12] D. J. Wigelsworth, B. A. Krantz, K. A. Christensen, D. B. Lacy, S. J. Juris, R. J. Collier, *J. Biol. Chem.* **2004**, *279*, 23349.
[13] R. M. Dawson, *J. Pharmacol. Toxicol. Methods* **2009**, *59*, 50.
[14] H. M. Scobie, J. A. Young, *Curr. Opin. Microbiol.* **2005**, *8*, 106.
[15] M. Y. Go, E. M. Chow, J. Mogridge, *Infect. Immun.* **2009**, *77*, 52.
[16] M. Y. Yang, A. Chaudhary, S. Seaman, J. Dunty, J. Stevens, M. K. Elzarrad, A. E. Frankel, B. St Croix, *Biochim. Biophys. Acta* **2011**, *1813*, 39.
[17] M. Jin, L. Andricioaei, T. A. Springer, *Structure* **2004**, *12*, 2137.
[18] J. D. Ramey, V. A. Villareal, C. Ng, S. C. Ward, J. P. Xiong, R. T. Clubb, K. A. Bradley, *Biochemistry* **2010**, *49*, 7403.
[19] M. J. Sippl, M. Wiederstein, *Bioinformatics* **2008**, *24*, 426.
[20] E. Santelli, L. A. Bankston, S. H. Leppla, R. C. Liddington, *Nature* **2004**, *430*, 905.
[21] A. Fiser, R. K. G. Do, A. Sali, *Protein Sci.* **2000**, *9*, 1753.
[22] B. R. Brooks, R. E. Bruccoleri, B. D. Olafson, D. J. States, S. Swaminathan, M. Karplus, *J. Comput. Chem.* **1983**, *4*, 187.
[23] A. D. MacKerell, D. Bashford, M. Bellott, R. L. Dunbrack, J. D. Evanseck, M. J. Field, S. Fischer, J. Gao, H. Guo, S. Ha, D. Joseph-McCarthy, L. Kuchnir, K. Kuczera, F. T. K. Lau, C. Mattos, S. Michnick, T. Ngo, D. T. Nguyen, B. Prodhom, W. E. Reiher, B. Roux, M. Schlenkrich, J. C. Smith,

R. Stote, J. Straub, M. Watanabe, J. Wiorkiewicz-Kuczera, D. Yin, M. Karplus, *J. Phys. Chem. B* **1998**, *102*, 3586.
[24] L. Wang, L. Li, E. Alexov, *Proteins* **2015**, *83*, 2186.
[25] J. C. Phillips, R. Braun, W. Wang, J. Gumbart, E. Tajkhorshid, E. Villa, C. Chipot, R. D. Skeel, L. Kale, K. Schulten, *J. Comput. Chem.* **2005**, *26*, 1781.
[26] S. Genheden, U. Ryde, *J. Comput. Chem.* **2011**, *32*, 187.
[27] J. A. Izaguirre, D. P. Catarello, J. M. Wozniak, R. D. Skeel, *J. Chem. Phys.* **2001**, *114*, 2090.
[28] G. J. Martyna, D. J. Tobias, M. L. Klein, *J. Chem. Phys.* **1994**, *101*, 4177.
[29] M. J. Harvey, G. De Fabritiis, *J. Chem. Theory Comput.* **2009**, *5*, 2371.
[30] A. P. Ruymgaart, R. Elber, *J. Chem. Theory Comput.* **2012**, *8*, 4624.
[31] T. Hou, J. Wang, Y. Li, W. Wang, *J. Chem. Inf. Model.* **2011**, *51*, 69.
[32] S. Genheden, U. Ryde, *J. Comput. Chem.* **2010**, *31*, 837.
[33] P. A. Greenidge, C. Kramer, J. C. Mozziconacci, R. M. Wolf, *J. Chem. Inf. Model.* **2013**, *53*, 201.
[34] A. R. Brice, B. N. Dominy, *J. Comput. Chem.* **2011**, *32*, 1431.
[35] D. Sitkoff, K. A. Sharp, B. Honig, *J. Phys. Chem.* **1994**, *98*, 1978.
[36] P. Ferrara, J. Apostolakis, A. Caflisch, *Proteins* **2002**, *46*, 24.
[37] W. Im, M. S. Lee, C. L. Brooks, III, *J. Comput. Chem.* **2003**, *24*, 1691.
[38] B. N. Dominy, C. L. Brooks, *J. Phys. Chem. B* **1999**, *103*, 3765.
[39] J. Chen, W. Im, C. L. Brooks, *III, J. Am. Chem. Soc.* **2006**, *128*, 3728.
[40] W. Im, M. Feig, C. L. Brooks, *Biophys. J.* **2003**, *85*, 2900.
[41] B. N. Dominy, C. L. Brooks, *Proteins* **1999**, *36*, 318.
[42] D. B. Lacy, D. J. Wigelsworth, H. M. Scobie, J. A. T. Young, R. J. Collier, *Proc. Natl. Acad. Sci. USA* **2004**, *101*, 6367.
[43] C. Petosa, R. J. Collier, K. R. Klimpel, S. H. Leppla, R. C. Liddington, *Nature* **1997**, *385*, 833.
[44] V. Zoete, M. Meuwly, M. Karplus, *Proteins* **2005**, *61*, 79.
[45] V. M. Gordon, K. R. Klimpel, N. Arora, M. A. Henderson, S. H. Leppla, *Infect. Immun.* **1995**, *63*, 82.
[46] D. J. Wigelsworth, B. A. Krantz, K. A. Christensen, D. B. Lacy, S. J. Juris, R. J. Collier, *J. Biol. Chem.* **2004**, *279*, 23349.
[47] P. F. Lang, B. C. Smith, *Dalton Trans.* **2010**, *39*, 7786.
[48] E. San Sebastian, J. M. Mercero, R. H. Stote, A. Dejaegere, F. P. Cossio, X. Lopez, *J. Am. Chem. Soc.* **2006**, *128*, 3554.
[49] A. D. Qu, D. J. Leahy, *Structure* **1996**, *4*, 931.
[50] E. F. Plow, T. A. Haas, L. Zhang, J. Loftus, J. W. Smith, *J. Biol. Chem.* **2000**, *275*, 21785.
[51] M. Shimaoka, T. Xiao, J. H. Liu, Y. T. Yang, Y. C. Dong, C. D. Jun, A. McCormack, R. G. Zhang, A. Joachimiak, J. Takagi, J. H. Wang, T. A. Springer, *Cell* **2003**, *112*, 99.
[52] J. Y. Lee, Y. M. Tsai, S. C. Chao, Y. F. Tu, *Clin. Exp. Dermatol.* **2005**, *30*, 176.
[53] J. O. Lee, P. Rieu, M. A. Arnaout, R. Liddington, *Cell* **1995**, *80*, 631.
[54] T. Vorup-Jensen, L. Chi, L. C. Gjelstrup, U. B. Jensen, C. A. Jewett, C. Xie, M. Shimaoka, R. J. Linhardt, T. A. Springer, *J. Biol. Chem.* **2007**, *282*, 30869.
[55] Y. Nymalm, J. S. Puranen, T. K. M. Nyholm, J. Kapyla, H. Kidron, O. T. Pentikainen, T. T. Airenne, J. Heino, J. P. Slotte, M. S. Johnson, T. A. Salminen, *J. Biol. Chem.* **2004**, *279*, 7962.
[56] J. Emsley, C. G. Knight, R. W. Farndale, M. J. Barnes, R. C. Liddington, *Cell* **2000**, *101*, 47.

Received: 16 August 2016
Revised: 8 January 2017
Accepted: 14 January 2017
Published online in Wiley Online Library